RECONSTRUCTION OF THE OCEANIC PRECIPITATION: PRELIMINARY RESULTS

Pingping Xie[1*], Mingyue Chen[1], John E. Janowiak[1], Phillip A. Arkin[2], and T.M. Smith[3)]

(1) NOAA / Climate Prediction Center, 5200 Auth Road, Camp Springs, MD 20746
(2) NOAA / Office of Global Programs, 1100 Wayne Ave., Suite 1210, Silver Springs, MD 20910-5603
(3) NOAA / National Climatic Data Center, 151 Patton Ave., Asheville, NC, 28801

1. INTRODUCTION

Efforts are underway in the NOAA Climate Prediction Center (CPC) to construct a global monthly precipitation analysis on a 2.5° latitude/longitude grid over the globe for an extended period from 1948 to the present. Over the global land areas, the analysis is defined by interpolating gauge observations of monthly precipitation, while over the global oceanic areas, it is produced by EOF reconstruction of the historical gauge observations over islands and land areas.

The construction of the monthly precipitation analysis over land has been completed for a 53-year period from 1948 to 2000 (Chen et al. 2001). The gauge-based analyses are now available through ftp (ftp.ncep.noaa.gov/pub/precip). The objective of this paper is to report the progress in defining the oceanic precipitation analysis by EOF reconstruction.

2. METHODOLOGY AND DATA

The oceanic precipitation analysis is defined by projecting historical gauge observations over islands and land areas onto EOF patterns determined from satellite-based precipitation estimates for later years using a technique applied successfully by Smith et al. (1996) in reconstruction of SST fields.

Assuming that there is no trend in precipitation throughout the target period and that the EOF structure of the precipitation for the target period is the same as that for the later period for which the satellite estimates are available, the oceanic precipitation anomaly (P) can be estimated through EOF reconstruction:

$$P(x,t) = \sum_{n=1}^{N} Sn(x) \cdot Tn(t) \quad \text{..... <1>}$$

Here, x, t, and n represent space grid point, time step, and EOF mode, respectively. Sn is the nth mode EOF spatial loading function for the satellite estimates. Tn is the time function for nth EOF mode and is determined by projecting the historical observations H onto spatial loading function Sn:

$$Tn(t) = \sum_{x=1}^{K} Sn(x) \cdot H(x,t) \quad \text{..... <2>}$$

To define the spatial loading function, satellite estimates of precipitation were derived from NOAA OLR data through the OLR-based Precipitation Index (OPI, Xie and Arkin 1998) for a 20-year period from 1979 to 1998. The gauge observations of monthly precipitation collected in Global Historical Climatology Network (GHCN, Version 2) of NOAA/NCDC and Climate Anomaly Monitoring Systems (CAMS) of NOAA/CPC are used here as historical data.

3. RECONSTRUCTION OVER THE GLOBAL DOMAIN

To examine the best strategy for the reconstruction and to get insight into how well the reconstructed fields may represent large-scale variability in precipitation, cross validation tests were conducted for the 20-year period from 1979 to 1998. The OPI data for a sub-period of two consecutive years were withdrawn and EOF analysis was performed for the OPI data for the remaining 18 years to get the spatial loading functions. Reconstructed fields were then computed by projecting the gauge data onto the EOF patterns derived for the 18-year period and compared with the OPI estimates for the 2-year withdrawn period. This process was repeated 10 times so that the entire 20-year period was covered by the cross validation.

In each cross validation test, two sets of reconstructions were created using different gauge data. In the first set, simulated gauge data is used by assuming that they are the same as the OPI estimates for grid boxes with at least one gauge and as missing for those with no gauges. In the second set, the gauge data are taken as the arithmetic mean of the real gauge observations available in the grid box. Comparison of the results based on the simulated and the real gauge data gives us an idea on how much the reconstruction might be improved by using better gauge data.

First, cross validation tests were conducted for reconstruction over the entire global domain (60°S-75°N). Reconstructions were conducted for the four 3-month seasons (DJF, MAM, JJA, and SON) separately to improve performance.

* Corresponding author address: Dr. Pingping Xie, NOAA / Climate Prediction Center, 5200 Auth Road, #605, Camp Springs, MD 20746, USA. E-mail: Pingping.Xie@noaa.gov

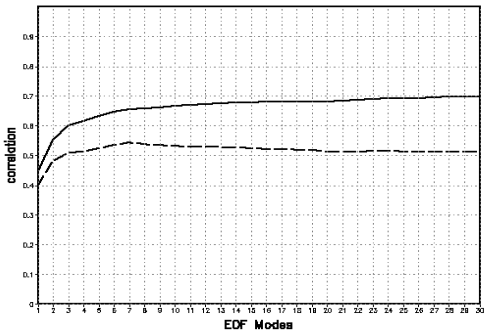

Fig. 1 Correlation between the oceanic monthly precipitation anomalies as observed in the withdrawn OPI estimates and those from the 2 sets of reconstructions using spatial loading functions of various numbers of EOF modes. Correlations were calculated over global oceanic areas from 60°S-60°N for DJF periods from 1979 to 1998. Results for reconstructions using simulated and real gauge data are plotted in solid and dashed lines, respectively.

As shown in fig.1, for the reconstruction using simulated gauge data (perfect historical data), the inclusion of more EOF modes always improves the agreement of the reconstructed anomaly fields, but changes in correlation are very small after more than 8 modes of EOF functions are used. The correlation is 0.45 for reconstruction using just 1 mode and reaches 0.65 when ~8 modes are included. For the reconstruction using real gauge data, the correlation improves as up to ~8 EOF modes are used. Adding more components associated with EOF modes higher than 8, however, yields little change in the correlation.

Based on these results, we decided to perform the reconstruction over the global domain using the first 8 modes of EOF spatial functions. Fig. 2 shows an example of the precipitation anomaly for January 1998 as obtained in the OPI estimates, the reconstructed fields using simulated and real gauge data. The anomaly pattern associated with ENSO is well represented in the reconstruction using both the simulated and real gauge data, over tropical Pacific, tropical Atlantic and eastern tropical Indian ocean. The agreement of the reconstructed anomaly with the withdrawn OPI estimates, however, is less desirable over the western tropical Indian ocean and over some of the extra-tropical areas.

To further understand the performance of the reconstructed anomaly fields in representing large-scale precipitation variability, components associated with ENSO and several major circulation patterns were examined. The circulation patterns examined here include the North Atlantic Oscillation (NAO), the Pacific / North American (PNA) mode, the Eastern Atlantic (EA) mode, the Western Pacific (WP) mode, and the Eastern

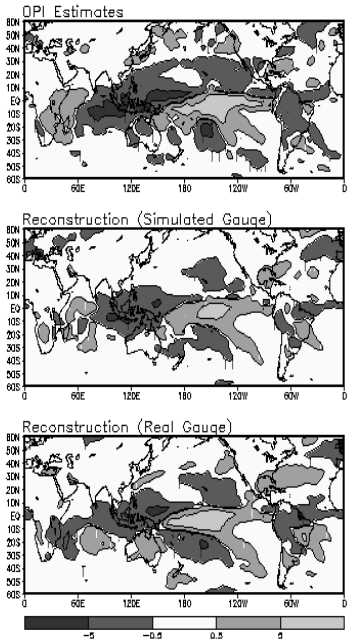

Fig.2 Precipitation anomaly (mm/day) for January 1998 as observed in the OPI estimates (top), reconstruction using simulated gauges (middle) and real gauges (bottom). The two sets of reconstructions are derived from cross validation tests.

Pacific (EP) mode (Barnston and Livezey, 1987).

First, components associated with ENSO and the selected circulation patterns were extracted for each grid box by taking linear regression between the precipitation anomalies and indices representing the climate patterns. Here, the NINO3 SST anomaly is used to represent ENSO while circulation indices of Barnston and Livezey (1987) are used to reflect time variations of the circulation patterns. Correlation between the components as retrieved from the constructed fields and those from the OPI estimates were then calculated. Table 1 presents results for the comparison over the global oceanic areas (60°S-60°N) for the DJF seasons.

As shown in Table 1, while the correlation for the total anomaly is 0.650 and 0.546, respectively, for reconstructions using simulated and real gauge data, the agreement in the anomaly components associated with ENSO and major circulation patterns are in general better, reaching over 0.7 for all patterns except the Eastern Pacific mode for reconstruction using simulated gauge data. This suggests that while the total precipitation anomaly is relatively difficult to extract, components associated with the major circulation patterns are reasonably well represented in the global reconstructions using 8 EOF modes.

Table 1: Correlation between the total anomaly and anomaly components associated with several major circulation patterns as observed in the OPI estimates and in the reconstructions over global oceanic areas (60°S-60°N) for DJF periods from 1979 to 1998. Results for reconstructions using simulated and real gauges are shown in the upper and bottom rows, respectively.

REC	TTL	ENSO	NAO	PNA	EA	WP	EP
SIMU	0.650	0.982	0.794	0.889	0.828	0.942	0.562
REAL	0.546	0.917	0.607	0.773	0.652	0.721	0.272

4. RECONSTRUCTION OVER REGIONAL DOMAINS

To explore the possibility of further improvements in the reconstructed fields, regional reconstructions were conducted for the residual anomaly fields of the global reconstructions using 8 EOF modes. Three regional domains were selected. These are the Atlantic Ocean (60°S-75°N), the North Pacific Ocean and the North Indian Ocean. In each case, nearby land areas are included as part of the regional domain to ensure reasonable availability of historical gauge data. For each regional domain, cross validation tests were conducted following the same procedures for the global reconstructions. Comparisons were made to evaluate the performance. Table 2 presents results for regional reconstruction over the Atlantic Ocean for the DJF seasons.

Table 2: Correlation between the total anomaly and anomaly components associated with several major circulation patterns as observed in the OPI estimates and in the reconstructions over Atlantic ocean for DJF periods from 1979 to 1998. Results for global reconstruction and global plus regional reconstruction using simulated gauge data are shown in upper and bottom rows, respectively.

REC	TTL	ENSO	NAO	PNA	EA	WP	EP
GLB	0.336	0.938	0.788	0.792	0.412	0.700	0.490
REG	0.459	0.941	0.911	0.847	0.723	0.737	0.612

Two things are clear from Table 2. While the reconstruction exhibits relatively low skill in retrieving total anomaly over the Atlantic Ocean, it is capable of extracting climate signals associated with ENSO and major circulation patterns there with reasonable accuracy. Performing regional reconstruction on the residual modes not used in the global reconstruction improves the quality of the reconstructed fields in representing most of the climate variation patterns to some extent.

5. SUMMARY

A series of cross validation tests have been conducted to examine the best strategy and the potential accuracy for oceanic precipitation reconstruction defined by projecting historical gauge observations over islands and land areas onto spatial functions derived from EOF analysis of the OPI estimates for a later period (1979-1998). The results showed that:

1) Using the first 8 EOF modes, the reconstruction over the entire global domain (60°S-75°N) is able to retrieve precipitation variation associated with ENSO and major large-scale circulation patterns with reasonable accuracy;

2) Performing regional reconstruction on the residual of the global reconstruction yields improvements to some extent for regions with reasonable gauge data;

Work is underway to modify the gauge data so that it can be better used to define the time function in the reconstruction. Once that task is finished, a test product of the reconstruction will be created and applied to verify model-produced precipitation fields for the period before 1980 when satellite estimates over ocean are not available.

REFERENCES

Barnston, A.G., and R.E. Livezey, 1987 : Classification, seasonality and persistence of low-frequency atmospheric circulation patterns. *Mon. Wea. Rev.*, **115**, 1083 - 1126.

Chen, M., P. Xie, J.E. Janowiak, P.A. Arkin, 2001: Global land precipitation: A 50-year monthly analysis based on gauge observations. *J. Hydrometeor.*, (in press).

Smith,T.M.,R.W.Reynolds, R.E. Livezey, and D.C. Stokes, 1996: Reconstruction of historical sea surface temperatures using empirical orthogonal functions. *J. Climate*, **9**, 1403-1420.

Xie, P., and P.A. Arkin, 1998: Global monthly precipitation estimates from satellite-observed outgoing longwave radiation. *J. Climate*, **11**, 137 - 164.